

Freezing of Gait Detection Using Gramian Angular Fields and Federated Learning from Wearable Sensors

Shovito Barua Soumma¹, S M Raihanul Alam², Rudmila Rahman³,
Umme Niraj Mahi⁴, Abdullah Mamun^{1,5}, Sayyed Mostafa Mostafavi¹,
Hassan Ghasemzadeh¹

¹College of Health Solutions, Arizona State University, Phoenix, AZ, USA

²Department of CSE, Bangladesh University of Engineering and Technology, Dhaka, Bangladesh

³Department of EEE, Bangladesh University of Engineering and Technology, Dhaka, Bangladesh

⁴Department of CSE, Khulna University of Engineering and Technology, Khulna, Bangladesh

⁵School of Computing and Augmented Intelligence, Arizona State University, Phoenix, AZ, USA

{shovito, a.mamun, smostaf3, hassan.ghasemzadeh}@asu.edu

{raihanul.hridoy100, rudmilar9, mahiummeniraj1}@gmail.com

Abstract

Freezing of gait (FOG) is a debilitating symptom of Parkinson's disease (PD) that impairs mobility and safety. Traditional detection methods face challenges due to intra and inter-patient variability, and most systems are tested in controlled settings, limiting their real-world applicability. Addressing these gaps, we present **FOGSense**, a novel FOG detection system designed for uncontrolled, free-living conditions. It uses Gramian Angular Field (GAF) transformations and federated deep learning to capture temporal and spatial gait patterns missed by traditional methods. We evaluated our FOGSense system using a public PD dataset, 'tdcsfog'. FOGSense improves accuracy by 10.4% over a single-axis accelerometer, reduces failure points compared to multi-sensor systems, and demonstrates robustness to missing values. The federated architecture allows personalized model adaptation and efficient smartphone synchronization during off-peak hours, making it effective for long-term monitoring as symptoms evolve. Overall, FOGSense achieves a 22.2% improvement in F1-score compared to state-of-the-art methods, along with enhanced sensitivity for FOG episode detection. Code is available: <https://github.com/shovito66/FOGSense>.

CCS Concepts

• **Computer systems organization** → **Sensor networks**;
• **Computing methodologies** → **Neural networks**; *Distributed algorithms*; • **Applied computing** → **Health informatics**.

Keywords

Wearable, Sensors, Federated Learning, CNN, Parkinson, Gait

1 Introduction

Approximately 90,000 people over the age of 65 are diagnosed with Parkinson's disease (PD) in the U.S. every year [32]. Freezing of Gait (FOG) is one of the most incapacitating symptoms of PD, a neurodegenerative condition that impairs coordination and mobility. The transient inability to start or continue walking, a hallmark of FOG, significantly impairs a patient's mobility and quality of life, increasing the risk of falls, accidents, and major health concerns [4, 15]. Therefore, timely detection of FOG and effective interventions can save a PD patient from severe injuries or even death. Timely treatments, including external cues or therapy changes, can help reduce falls, increase mobility, and improve the overall quality of life when FOG is detected early [1]. Additionally, real-time detection and ongoing monitoring could keep a doctor well-informed and help modify treatment regimens, which can lessen the frequency and intensity of FOG episodes [2].

The integration of wearable technologies with machine learning (ML) represents a major advancement in the continuous monitoring and management of PD symptoms. This convergence enables real-time motion pattern recognition, predictive modeling of FOG episodes, and personalized therapeutic insights. Conventional time series frameworks, however, struggle to capture the complex spatiotemporal dynamics and variability in patient movement, limiting their effectiveness in processing the multivariate data streams required for real-time FOG prediction and intervention [25, 31].

Wearable FOG detection systems also face challenges in sensor reliability and robustness. Sensor failures in mobile health monitoring can decrease detection accuracy by up to 65% when using conventional imputation methods [19]. This vulnerability is especially critical in systems relying on multiple sensors or data axes, where each dependency increases the risk of system failure in real-world deployments [19].

The Gramian Angular Field (GAF) transformation is a signal processing technique for FOG detection, commonly used with accelerometer and gyroscope data. By converting temporal sequences into 2D representations, GAF improves FOG detection with Convolutional Neural Networks (CNN) [7]. It outperforms wavelet and recurrence plot analysis by preserving local and global patterns while maintaining order [31]. Mapping data to polar coordinates in the Gramian matrix, GAF captures locomotor perturbations, and its 2D CNN approach extracts richer features than 1D CNNs, boosting FOG detection accuracy [13, 18].

To further investigate and enhance the efficacy of GAF and CNN for FOG detection, we designed FOGSense, a novel framework for FOG episode detection using only one axis of a single accelerometer sensor. This minimalist approach reduces hardware dependencies and enhances reliability while maintaining strong detection capabilities. By applying GAF transformations with a CNN, FOGSense enables both window-level and episode-level FOG detection. It effectively captures essential gait signatures within brief time windows, allowing for real-time use on resource-limited devices with low computational demand. Additionally, its single-axis design and dynamic weight transfer method improve precision and resilience against sensor failures.

Subsequently, we take another step to improve FOGSense by integrating federated learning. Modern smartphones can train models on-device but often strain battery and CPU [11, 34]. FOGSense overcomes this by employing a distributed learning framework tailored for wearable-smartphone ecosystems [12, 30]. In this setup, sensor data is transferred during off-peak hours to capture FOG patterns without interrupting regular use [21]. A central server then uses TensorFlow to train models, converts them to TensorFlow Lite for deployment, and adapts these models to both individual and population-wide FOG variations [14, 17, 20, 26]. This approach is optimized for resource-constrained devices [20], with asynchronous updates that balance performance and efficiency [34].

In summary, our contributions are (i) a review of FOG detection methods and challenges, (ii) a FOG detection solution using GAF, CNN, and federated learning with a single accelerometer, (iii) the development and evaluation of the FOGSense system for window-level, episode-level, and federated FOG detection, (iv) performance comparison across channels and with existing methods, and (v) a dynamic weight transfer framework to address channel failure.

2 Related Work

Recent advancements in FOG detection address the challenges of traditional sensor-based ML methods, with key directions being (1) raw sensor-based deep learning, (2) self-supervised learning (SSL), and (3) federated learning.

Raw sensor-based deep learning minimizes manual feature engineering by applying models like 1D-CNNs directly to accelerometer data [9, 36]. These methods reduce pre-processing overhead but require large labeled datasets and often fail to capture the full complexity of sensor signals. Moreover, they struggle with generalizability, particularly when faced with variations in patient populations or sensor placements [28], limiting their real-world applicability.

SSL techniques aim to overcome labeled data constraints by learning meaningful representations from raw data [29, 33]. These methods extract essential features without extensive annotation but face challenges in adapting to diverse sample distributions. Variations in environmental conditions, sensor noise, and individual gait patterns can significantly affect performance [16], highlighting the need for robust adaptation mechanisms.

Federated learning enables collaborative model training across devices while preserving data privacy [6, 14]. This distributed approach is particularly suitable for healthcare but presents challenges in resource-constrained wearables, such as balancing computational efficiency, power consumption, and model performance.

Building on these foundations, our work integrates GAF transformation with multichannel CNNs for enhanced feature extraction, surpassing traditional raw sensor-based approaches. Additionally, our federated learning implementation improves model adaptability while preserving privacy and addressing efficiency challenges, making it suitable for resource-constrained real-world applications.

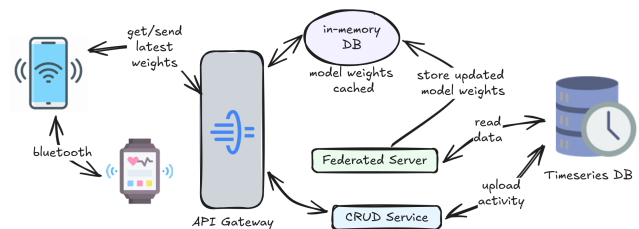


Figure 1: Proposed distributed federated system design.

3 FOGSense System Design

3.1 Federated Learning on Edge Devices

Developing a reliable FOG detection model is challenging due to the complexity of PD and symptom variability across patients. Our hierarchical system architecture, illustrated in Fig. 1, addresses these challenges while accommodating the constraints of wearable devices. Wearables continuously collect acceleration data, which is transferred to paired smartphones at designated intervals. A central federated server aggregates this data during off-peak hours, applies GAF transformations, and executes model training. The processed data are stored in a time-series database for comprehensive health

monitoring and temporal analysis. Updated model weights are saved in an in-memory database for efficient synchronization with smartphones, which then update wearables. This design ensures efficient data handling, robust model distribution, and reliable FOG monitoring.

3.2 Dataset

We used the publicly available PD dataset [10] from the TLVMC FOG prediction competition. The dataset has 62 subjects diagnosed with Parkinson’s disease, specifically, focusing on FOG episodes. The analysis concentrated on the ‘tdcsfog’ dataset. Data were collected via a lower-back triaxial accelerometer at 128 Hz, capturing vertical (AccV), mediolateral (AccML), and anteroposterior (AccAP) movements, critical for identifying directional mobility loss during FOG events. Rich temporal annotations, including start hesitations, turns, and walking, enabled precise FOG analysis. Using DHWT the FOG window counts rose from 1,096,265 to 1,994,705, yielding an 82% increase.

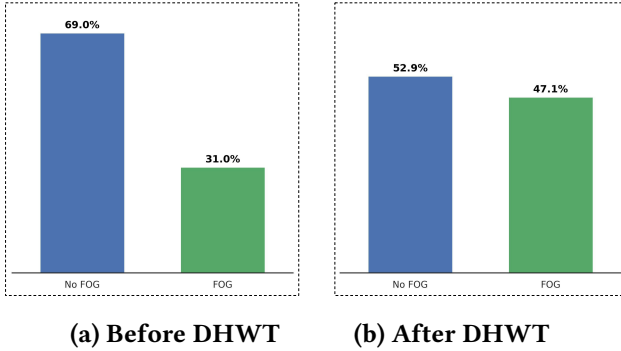


Figure 3: Class distribution normal and FOG events before (a) and after (b) applying *Differential Hopping Windowing Technique* (DHWT).

3.3 Pre-processing

The dataset, originally collected at 128Hz, was downsampled to 64Hz to reduce computational complexity while preserving signal characteristics [29]. The ‘tdcsfog’ data’s three event types were consolidated into a single column, labeling FOG as 1 and no-FOG as 0.

A critical preprocessing step involved defining time windows for analysis, which we set at 4-second intervals to effectively capture essential gait features for FOG detection [23]. To address class imbalance effectively, we incorporated the **Differential Hopping Windowing Technique (DHWT)**[29]. This technique applied varying overlap sizes: no overlap (0%) for no-FOG windows and an increased 50% overlap for FOG windows. By using this method, we enhanced the representation of FOG events, mitigating class imbalance and enriching the model’s training dataset without additional preprocessing. Fig 3 illustrates the results achieved

with this approach, showing a more balanced distribution of FOG and no-FOG instances. We filtered out impure windows where no-FOG events (class 0) predominated, designating windows where FOG events (class 1) were in the majority as pure FOG windows. For improved data consistency and distribution, we subtracted the mean value from each window ($X'_{i,j} = X_{i,j} - \mu_{X_i}$), ensuring normalization across samples.

Our methodology employs Conv2D CNN for FOG episode detection. To leverage CNNs’ proven capabilities in image processing, we transformed our temporal acceleration data into image-based representations using the GAF method. This transformation encodes temporal dependencies into a higher-dimensional space, allowing the CNN architecture to potentially capture complex patterns that might be less apparent in the original time series format.

3.4 Gramian Angular Fields

The GAF transformation effectively converts 1D time series data into 2D images suitable for CNN-based analysis while preserving temporal and dynamic structures [35]. The transformation process consists of two key steps: normalization and polar coordinate mapping. First, the time series data is normalized to the range $[-1, 1]$ through the following transformations:

$$x'_i = \frac{x_i - \min(X)}{\max(X) - \min(X)} \quad \theta_i = \cos^{-1}(x'_i) \quad (1)$$

$$x''_i = 2x'_i - 1 \quad r_i = \frac{t_i}{N} \quad (2)$$

where t_i represents the time stamp and N denotes the total number of points.

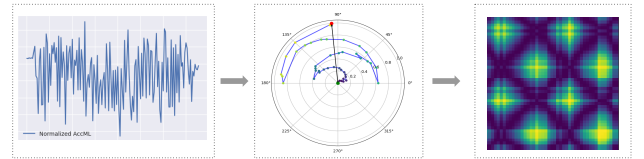


Figure 4: GAF transformation of accelerometer signals.

Figure 4: GAF transformation of accelerometer signals.

The next stage in the GAF process involves creating the Gram matrix, which captures temporal correlations between different time points using trigonometric functions. Specifically, for the Gramian Angular Summation Field (GASF), we compute:

$$\text{GASF}(i, j) = \cos(\theta_i + \theta_j) \quad (3)$$

For a time series of m data points, the resulting GASF matrix takes the form:

$$\text{GAF} = \begin{bmatrix} \cos(\theta_1 + \theta_1) & \cdots & \cos(\theta_1 + \theta_m) \\ \vdots & \ddots & \vdots \\ \cos(\theta_m + \theta_1) & \cdots & \cos(\theta_m + \theta_m) \end{bmatrix} \quad (4)$$

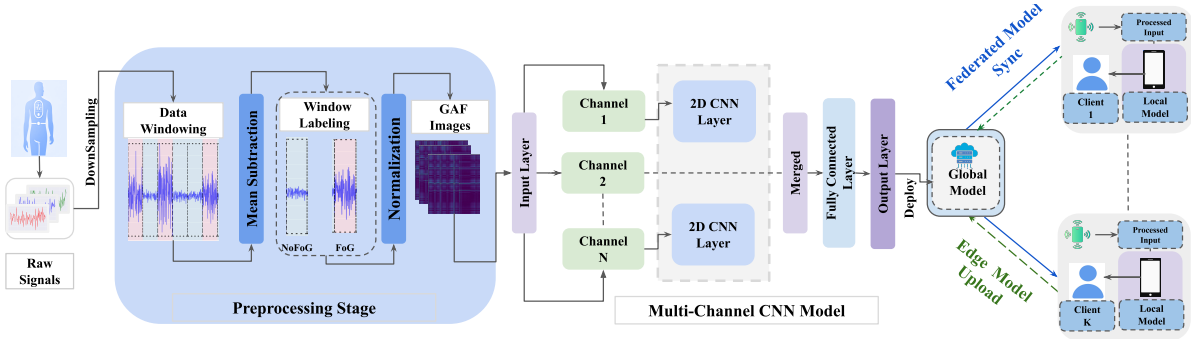


Figure 2: System architecture illustrating the federated learning workflow: local models are trained and uploaded by devices, then aggregated into a global model, which is distributed back to each device.

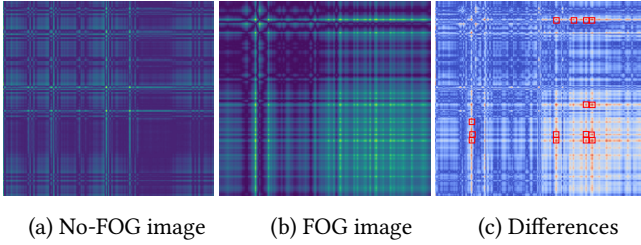


Figure 5: GAF-transformed images for (a) No-FOG, (b) FOG conditions, and (c) differences, with significantly different regions highlighted with red boxes.

As shown in Fig. 5, the GAF transformation creates distinct visual patterns for normal (Fig. 5a) and FOG (Fig. 5b) conditions, enabling image-based deep learning applications. The annotated difference, based on pixel-wise absolute differences between GAF-transformed images, highlights areas with significant pattern variations, capturing subtle gait changes. The top 15 regions with the highest difference values are emphasized, showcasing where the FOG pattern deviates most from no-FOG. This approach effectively captures temporal patterns in sequential data, making it ideal for medical signal processing and gait analysis [5].

3.5 Dataset Stratification

We used subject-based stratified partitioning to prevent data leakage and ensure robust evaluation [27]. The dataset was split into training (70%), validation (10%), and testing (20%) sets using randomly shuffled subject identifiers and it preserved FOG/no-FOG proportions and temporal integrity [8]. This procedure is repeated for each group within the dataset, conducted three times, and the results are averaged to ensure reliability and robustness in our findings.

3.6 Experimental Setup

Our FOG detection system employs a sophisticated multichannel 2D Convolutional Neural Network (CNN) architecture designed to maximize performance through spatial

relationship analysis across multiple sensor modalities. The architecture processes data from three distinct accelerometer axes—Vertical (AccV), Mediolateral (AccML), and Antero-posterior (AccAP)—by transforming them into GAF images and processing them through dedicated CNN branches. This approach enables the system to leverage complementary information from different sensor perspectives, significantly enhancing its FOG detection capabilities.

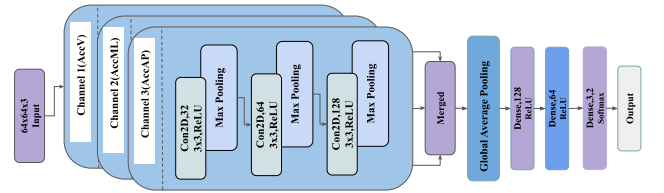


Figure 6: The multichannel CNN architecture.

The proposed architecture, as illustrated in Fig. 6, consists of three parallel CNN branches, each dedicated to processing GAF images from a specific accelerometer axis. Each branch processes input data with dimensions (64, 64, 3) through three consecutive convolutional blocks of increasing complexity. The first block utilizes 32 filters with 20% dropout,

Table 1: Dense layers after feature concatenation.

Layer	Units	Regularization	Dropout
First Dense	128	L2 ($\lambda = 0.001$)	40%
Second Dense	64	None	20%
Output Dense	2	None	None

while the second and third blocks employ 64 and 128 filters respectively, incorporating L2 regularization ($\lambda = 0.001$) and increasing dropout rates (20% and 40%). Each convolutional block integrates batch normalization and max pooling operations to enhance feature learning and reduce spatial dimensions. A global average pooling layer follows the convolutional blocks, effectively reducing parameters while capturing essential global features from each branch.

Features extracted from individual branches are concatenated to create a unified representation, which then passes through two dense layers for final classification. The first dense layer comprises 128 neurons with ReLU activation, L2 regularization ($\lambda = 0.001$), and 40% dropout, followed by a second dense layer of 64 neurons with ReLU activation and 20% dropout. The final classification is performed by a softmax layer with two neurons corresponding to FOG and no-FOG classes. To ensure robust performance and prevent overfitting, the model incorporates multiple regularization techniques Adam optimizer with the categorical cross-entropy loss function. The backbone architecture remained unchanged during channel configuration analysis, ensuring performance differences stemmed solely from input channel variations.

Finally, we also proposed a dynamic weight transfer mechanism to handle the failure of any sensor channel. As the architecture is the same for each channel, when a channel fails, the system can load the weights for a different functional channel and predict with that channel. For example, if the channel AccV fails at any time and the channel AccAP is functional, the FOGSense system will load the weights trained with AccAP and make the prediction. This is shown in Algorithm 1.

FOGSense was evaluated using standard binary classification metrics. Based on the confusion matrix elements—true positives (TP), false positives (FP), false negatives (FN), and true negatives (TN)—we computed the following metrics: sensitivity, precision, accuracy, and F1-score.

Algorithm 1 Inference with Dynamic Weight Transfer

- 1: **Training and testing before deployment:**
 - 2: Train N models of identical architecture separately for N channels and evaluate them on the test dataset.
 - 3: Sort the N models and channels in descending order of their test F-1 scores as:

$$\text{Models} = (\text{Model}_1, \text{Model}_2, \dots, \text{Model}_N)$$

$$\text{Channels} = (\text{Channel}_1, \text{Channel}_2, \dots, \text{Channel}_N)$$
 - 4: Save the weights of all models.
 - 5: **Inference after deployment:**
 - 6: Find the smallest i such that Channel_i is functional in new data.
 - 7: Load weights of Model_i .
 - 8: Predict using the i -th channel’s readings in the new data.
-

4 Results

Our experiments excluded conventional data augmentation to preserve GAF signal integrity. We evaluated window-level and temporal FOG detection, achieving promising results. To enhance clinical applicability, we used federated learning for continuous model adaptation, preserving privacy and enabling model refinement across edge devices.

Table 2: FOGSense’s performance for three different detection types using all three channels. DFW: Detected FOG Windows, DFE: Detected FOG Episodes.

Detection Type	Configuration	Accuracy (%)	F1 (%)
Window-level (DFW)	All Channels	87.23	90.31
Episode-level (DFE)	All Channels	87.23	90.86
Federated Learning	All Channels	86.98	90.47

4.1 Effect of Channel Selection

We conducted a systematic evaluation of input channel configurations to optimize our FOG detection framework. Initially utilizing all three accelerometer axes (anterior-posterior, mediolateral, and vertical), we investigated the impact of channel reduction on model performance. The analysis focused on quantifying the trade-off between computational efficiency and FOG detection accuracy across different channel combinations to determine the optimal configuration. Here, each model was trained for 60 epochs.

Table 3: Impact of selection of AccV (Vertical), AccML (Mediolateral), and AccAP (Anteroposterior) axes.

Channels	Input Combination	Duration (s/epoch)		ACC	F1	PRE	SEN
		Train	Test				
3	AccAP-AccML-AccV	63.0	12.9	87.2	90.3	90.3	91.0
	AccAP-AccML	32.1	15.4	93.2	87.7	93.2	93.2
2	AccML-AccV	31.8	19.0	95.3	90.8	95.3	95.3
	AccAP-AccV	31.7	13.3	94.5	90.5	94.5	94.5
1	AccAP	11.3	11.0	93.2	93.0	93.2	93.2
	AccML	17.7	19.0	89.2	83.0	89.2	89.2
	AccV	11.3	11.0	96.3	96.3	95.8	96.3

Table 3 reveals several key insights regarding channel configuration impact on model performance. The baseline three-channel configuration (AccAP-AccML-AccV) achieved 87.23% accuracy and 90.31% F1-score, requiring 63 seconds per training epoch. However, reducing to two channels generally improved performance while halving the training time to approximately 32 seconds per epoch. Among dual-channel configurations, AccML-AccV demonstrated superior performance with 95.30% accuracy and 90.75% F1-score.

Notably, single-channel configurations further reduced training time to approximately 11 seconds per epoch while maintaining or improving performance. The AccV channel alone achieved the highest overall accuracy of 96.25% and F1-score of 96.27%, surpassing both three-channel and two-channel configurations. In contrast, AccML showed a relatively lower performance (89.24% accuracy), while AccAP maintained a robust performance (93.24% accuracy).

As illustrated in Fig. 7, the single AccV channel configuration (highlighted in red) emerges as the optimal choice, offering superior performance metrics while minimizing computational overhead. This finding suggests that AccV

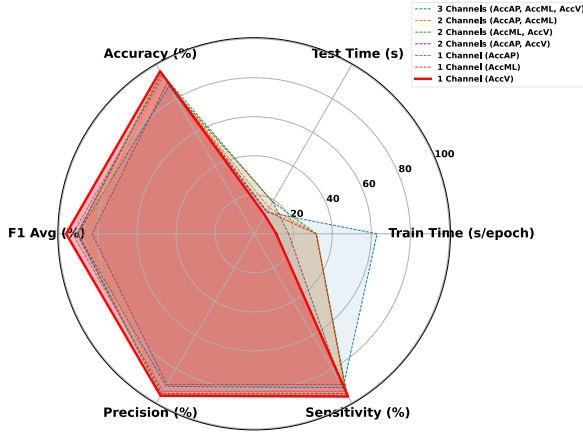


Figure 7: Comparison of channel configurations in the FOGSense system shows that the vertical axis (AccV) obtains a better F1 score than other channel choices.

alone captures sufficient information for effective FOG detection, making it particularly suitable for resource-constrained applications. Additionally, this configuration is resilient to missing values, as it continues to perform effectively even when data from other axes is unavailable, achieving better results using only the AccV channel.

4.2 Comparison with State-of-the-Art

We present a comparative analysis of FOGSense and the other state-of-the-art (SOTA) methods in Table 4. Our FOGSense method achieves an F1 score of 0.96 on the ‘tdcsfog’ dataset, whereas the closest competitor LIFT-PD achieved an F1 score of 0.79. Moreover, unlike the other methods, the FOGSense maintains a score of at least 0.90 in all four metrics. Additionally, FOGSense’s use of the vertical axis (AccV) channel selection not only enhances detection accuracy but also provides a more efficient approach to gait monitoring. These results underscore FOGSense’s potential as a powerful and dependable tool for real-time gait analysis.

Table 4: FOGSense vs. state-of-the-art on *tdcsfog*. The best values for each metric are highlighted in bold, while the second-best values are underlined.

Study	DFE	SEN (DFW)	PRE	F1
One Class Classifier [24]	90.8%	71.6%	<u>0.86</u>	0.77
Semi-Supervised Model [22]	–	72.3%	–	–
Multi-head CNN [3]	97.3%	<u>94.6%</u>	0.56	0.68
LIFT-PD	88%	<u>84%</u>	0.74	<u>0.79</u>
FOGSense	–	96.3%	0.958	0.963

5 Discussion

In this paper, we introduced a novel approach to detect FOG by integrating GAF-transformed accelerometer data with a multichannel CNN architecture and a decentralized federated

learning pipeline. Our experiments demonstrated not only high detection accuracy but also highlighted the practicality of our system for real-world deployment. A key finding is that a single-channel configuration using only the vertical acceleration component (AccV) achieved impressive performance—96.25% accuracy and 96.27% F1-score—while significantly reducing computational demands compared to multi-channel configurations. This result challenges the traditional view that multiple sensor channels are essential for accurate FOG detection.

To address continuous monitoring constraints, we developed a distributed framework that synchronizes data between wearable devices and smartphones during off-peak hours, balancing the demands of monitoring, battery life, and computational efficiency. Although the GAF transformation was effective in our approach, exploring alternative time series representations such as Recurrence Plots and Markov Transition Fields may yield further insights. Additionally, while our distributed framework shows promise in simulations, real-world validation on multiple devices is a critical next step. Investigating different weight calculation methods beyond weighted averaging could enhance the learning dynamics in federated learning. Testing the model across diverse patient populations and datasets would further strengthen its generalizability, and studying patient data mixing strategies may provide insights into managing individual gait variations effectively.

6 Conclusion

Accurate detection of freezing of gait (FOG) can significantly enhance early intervention strategies, improve mobility support, and ultimately contribute to a better quality of life for individuals with Parkinson’s disease. Our FOGSense system uses Gramian Angular Field (GAF) imaging, convolutional neural networks (CNN), and federated learning to ensure accurate and resource-efficient FOG detection in an uncontrolled environment. Moreover, FOGSense is robust to sensor failure as it needs only one channel to make an accurate prediction and it can delegate the prediction task to a different single-channel model by dynamic weight transfer in case of a channel failure.

Our work establishes a foundation for efficient, practical, and reliable FOG detection systems. We provide new insights into lightweight, single-channel solutions that outperform state-of-the-art multi-channel solutions. We also identified future research directions that could advance the field, from alternative data representations to federated learning enhancements and real-world validations. This study highlights the potential of FOGSense and opens avenues for refining FOG detection systems to meet clinical and practical demands more effectively.

References

- [1] Claas Ahlrichs, Albert Samà, Michael Lawo, Joan Cabestany, Daniel Rodríguez-Martín, Carlos Pérez-López, Dean Sweeney, Leo R Quinlan, Gearóid Ó Laighin, Timothy Counihan, et al. 2016. Detecting freezing of gait with a tri-axial accelerometer in Parkinson's disease patients. *Medical & biological engineering & computing* 54 (2016), 223–233.
- [2] Luigi Borzi, Ivan Mazzetta, Alessandro Zampogna, Antonio Suppa, Gabriella Olmo, and Fernanda Irrera. 2021. Prediction of freezing of gait in Parkinson's disease using wearables and machine learning. *Sensors* 21, 2 (2021), 614.
- [3] Luigi Borzi, Luis Sigcha, Daniel Rodríguez-Martín, and Gabriella Olmo. 2023. Real-time detection of freezing of gait in Parkinson's disease using multi-head convolutional neural networks and a single inertial sensor. *Artif. Intell. Med.* 135, C (jan 2023), 13 pages. <https://doi.org/10.1016/j.artmed.2022.102459>
- [4] Jan Brederbecke. 2023. Freezing of Gait Prediction From Accelerometer Data Using a Simple 1D-Convolutional Neural Network–8th Place Solution for Kaggle's Parkinson's Freezing of Gait Prediction Competition. *arXiv preprint arXiv:2307.03475* (2023).
- [5] Aybüke Cvrızoğlu Buz, Mustafa Umüt Demirezen, and Uraz Yavanoğlu. 2020. A novel approach and application of time series to image transformation methods on classification of underwater objects. *Gazi Mühendislik Bilimleri Dergisi* 7, 1 (2020), 1–11.
- [6] Yiqiang Chen, Xin Qin, Jindong Wang, Chaohui Yu, and Wen Gao. 2020. Fedhealth: A federated transfer learning framework for wearable healthcare. *IEEE Intelligent Systems* 35, 4 (2020), 83–93.
- [7] Youssef Elmir, Yassine Himeur, and Abbes Amira. 2023. ECG classification using deep CNN and Gramian angular field. In *2023 IEEE Ninth International Conference on Big Data Computing Service and Applications (BigDataService)*. IEEE, 137–141.
- [8] Nils Y Hammerla, Shane Halloran, and Thomas Plötz. 2016. Deep, convolutional, and recurrent models for human activity recognition using wearables. *arXiv preprint arXiv:1604.08880* (2016).
- [9] Julius Hannink, Thomas Kautz, Cristian F Pasluosta, Karl-Günter Gaßmann, Jochen Klucken, and Bjoern M Eskofier. 2016. Sensor-based gait parameter extraction with deep convolutional neural networks. *IEEE journal of biomedical and health informatics* 21, 1 (2016), 85–93.
- [10] Addison Howard, amit salomon, eran gazit, Jeff Hausdorff, Leslie Kirsch, Maggie, Pieter Ginis, Ryan Holbrook, and Yasir F Karim. 2023. Parkinson's Freezing of Gait Prediction. <https://kaggle.com/competitions/tlvmc-parkinsons-freezing-gait-prediction>. Kaggle.
- [11] Andrey Ignatov, Radu Timofte, William Chou, Ke Wang, Max Wu, Tim Hartley, and Luc Van Gool. 2019. AI Benchmark: Running deep neural networks on Android smartphones. In *Proceedings of the European Conference on Computer Vision (ECCV) Workshops*. 0–0.
- [12] Latif U Khan, Shashi Raj Pandey, Nguyen H Tran, Walid Saad, Zhu Han, Minh NH Nguyen, and Choong Seon Hong. 2020. Federated learning for edge networks: Resource optimization and incentive mechanism. *IEEE Communications Magazine* 58, 10 (2020), 88–93.
- [13] Trung-Hieu Le, Thai-Khanh Nguyen, Trung-Kien Tran, Thanh-Hai Tran, and Cuong Pham. 2023. GAFormer: Wearable IMU-Based Human Activity Recognition with Gramian Angular Field and Transformer. In *2023 Asia Pacific Signal and Information Processing Association Annual Summit and Conference (APSIPA ASC)*. IEEE, 297–303.
- [14] Tian Li, Anit Kumar Sahu, Ameet Talwalkar, and Virginia Smith. 2020. Federated learning: Challenges, methods, and future directions. *IEEE signal processing magazine* 37, 3 (2020), 50–60.
- [15] David Gordon Lichter, Ralph Holmes Boring Benedict, and Linda Ann Hershey. 2021. Freezing of gait in Parkinson's disease: risk factors, their interactions, and associated nonmotor symptoms. *Parkinson's Disease* 2021, 1 (2021), 8857204.
- [16] Luca Lonini, Andrew Dai, Nicholas Shawen, Tanya Simuni, Cynthia Poon, Leo Shimanovich, Margaret Daeschler, Roozbeh Ghaffari, John A Rogers, and Arun Jayaraman. 2018. Wearable sensors for Parkinson's disease: which data are worth collecting for training symptom detection models. *NPJ digital medicine* 1, 1 (2018), 64.
- [17] Jun Luo, Bing Song, Ming Wen, Hui Dong, and Yanan Zhang. 2020. HFL: Hybrid federated learning for healthcare applications on edge devices. In *2020 IEEE International Conference on Big Data (Big Data)*. IEEE, 3172–3181.
- [18] Edson F Luque Mamani and Cristian Lopez del Alamo. 2019. Gaf-cnn-1stm for multivariate time-series images forecasting. In *LatinX in AI Research at ICML 2019*.
- [19] Abdullah Mamun, Seyed Iman Mirzadeh, and Hassan Ghasemzadeh. 2022. Designing Deep Neural Networks Robust to Sensor Failure in Mobile Health Environments. In *2022 44th Annual International Conference of the IEEE Engineering in Medicine & Biology Society (EMBC)*. IEEE, 2442–2446.
- [20] Akhil Mathur, Aarno Isopoussu, Fahim Kariluoma, Sasu Tarkoma, Matti Jain, and Deborah Estrin. 2017. Deepeye: Resource efficient local execution of multiple deep vision models using wearable commodity hardware. In *Proceedings of the 15th Annual International Conference on Mobile Systems, Applications, and Services*. 68–81.
- [21] Sinziana Mazilu, Ulf Blanke, Alberto Calatroni, Eran Gazit, Jeffrey M Hausdorff, and Gerhard Tröster. 2015. Prediction of freezing of gait in Parkinson's from physiological wearables: an exploratory study. In *Journal of Parkinson's disease*, Vol. 5. IOS Press, 229–236.
- [22] Val Mikos, Chun-Huat Heng, Arthur Tay, Nicole Shuang Yu Chia, Karen Mui Ling Koh, Dawn May Leng Tan, and Wing Lok Au. 2017. Real-time patient adaptivity for freezing of gait classification through semi-supervised neural networks. In *2017 16th IEEE International Conference on Machine Learning and Applications (ICMLA)*. IEEE, 871–876.
- [23] Nader Naghavi and Eric Wade. 2019. Prediction of freezing of gait in Parkinson's disease using statistical inference and lower-limb acceleration data. *IEEE transactions on neural systems and rehabilitation engineering* 27, 5 (2019), 947–955.
- [24] Nader Naghavi and Eric Wade. 2021. Towards real-time prediction of freezing of gait in patients with Parkinson's disease: a novel deep one-class classifier. *IEEE Journal of Biomedical and Health Informatics* 26, 4 (2021), 1726–1736.
- [25] Scott Pardoel, Jonathan Kofman, Julie Nantel, and Edward D Lemaire. 2019. Wearable-sensor-based detection and prediction of freezing of gait in Parkinson's disease: a review. *Sensors* 19, 23 (2019), 5141.
- [26] Nicola Rieke, Jonny Hancox, Wenqi Li, Fausto Milletari, Holger R Roth, Shadi Albarqouni, Spyridon Bakas, Mathieu N Galtier, Bennett A Landman, Klaus Maier-Hein, et al. 2020. The future of digital health with federated learning. *NPJ digital medicine* 3, 1 (2020), 1–7.
- [27] Sohrab Saeb, Luca Lonini, Arun Jayaraman, David C Mohr, and Konrad P Kording. 2017. Scalable brain-computer interface (BCI) cross-validation requires subject-wise partitioning. *Journal of neural engineering* 14, 4 (2017), 046017.
- [28] Albert Sama, Carlos Pérez-López, Jaume Romagosa, D Rodríguez-Martín, Andreu Catala, Joan Cabestany, David A Perez-Martinez, and Alejandro Rodríguez-Molinero. 2012. Dyskinesia and motor state detection in Parkinson's disease patients with a single movement sensor. In *2012 Annual International Conference of the IEEE Engineering in Medicine and Biology Society*. IEEE, 1194–1197.
- [29] Shovito Barua Soumma, Kartik Mangipudi, Daniel Peterson, Shyamal Mehta, and Hassan Ghasemzadeh. 2024. Self-Supervised Learning and Opportunistic Inference for Continuous Monitoring of Freezing of Gait in Parkinson's Disease. *arXiv preprint arXiv:2410.21326* (2024).

- [30] Xiaofei Wang, Yiwen Han, Chenyang Wang, Qiyang Zhao, Xu Chen, and Min Chen. 2020. Convergence of edge computing and deep learning: A comprehensive survey. *IEEE Communications Surveys & Tutorials* 22, 2 (2020), 869–904.
- [31] Zhiguang Wang and Tim Oates. 2015. Imaging time-series to improve classification and imputation. *arXiv preprint arXiv:1506.00327* (2015).
- [32] AW Willis, E Roberts, JC Beck, B Fiske, W Ross, R Savica, SK Van Den Eeden, CM Tanner, C Marras, and Parkinson’s Foundation P4 Group Alcalay Roy Schwarzschild Michael Racette Brad Chen Honglei Church Tim Wilson Bill Doria James M. 2022. Incidence of Parkinson disease in North America. *npj Parkinson’s Disease* 8, 1 (2022), 170.
- [33] Yi Xia, Hua Sun, Baifu Zhang, Yangyang Xu, and Qiang Ye. 2024. Prediction of freezing of gait based on self-supervised pretraining via contrastive learning. *Biomedical Signal Processing and Control* 89 (2024), 105765.
- [34] Qiang Yang, Yang Liu, Tianjian Chen, and Yongxin Tong. 2019. Federated learning in mobile edge networks: A comprehensive survey. *IEEE Communications Surveys & Tutorials* 22, 3 (2019), 2031–2063.
- [35] Umaporn Yokkampon, Abbe Mowshowitz, Sakmongkon Chumkamon, and Eiji Hayashi. 2022. Autoencoder with Gramian Angular Summation Field for Anomaly Detection in Multivariate Time Series Data. *Journal of Advances in Artificial Life Robotics* 2, 4 (2022), 206–210.
- [36] Aite Zhao, Lin Qi, Jie Li, Junyu Dong, and Hui Yu. 2018. A hybrid spatio-temporal model for detection and severity rating of Parkinson’s disease from gait data. *Neurocomputing* 315 (2018), 1–8.